THE JOURNAL OF PHYSICAL CHEMISTRY B

Article

Cite This: J. Phys. Chem. B 2019, 123, 8057−8064

pubs.acs.org/JPCB

Promotion Effect of Succinimide on Amyloid Fibrillation of Hen Egg-White Lysozyme

Wei Fan,[†] Lei Xing,[†] Ning Chen,[†] Xiaoguo Zhou,*[,†] Yuanqin Yu,*[,‡] and Shilin Liu*[,†]

[†]Hefei National Laboratory for Physical Sciences at the Microscale, iChEM (Collaborative Innovation Center of Chemistry for Energy Materials), Department of Chemical Physics, University of Science and Technology of China, Hefei, Anhui 230026, China

[‡]Department of Physics, Anhui University, Hefei, Anhui 230601, China

Supporting Information

ABSTRACT: Amyloid fibrillation is closely associated with a series of neurodegenerative diseases. According to that, the intermediate soluble oligomers and protofibrils are more toxic; reducing their concentrations in protein solutions by accelerating fibrillation is believed as a feasible strategy for treatment or remission of the diseases. Using hen egg-white lysozyme (HEWL) as a model protein, the promotion effect of succinimide was revealed by a series of experiments, e.g., atomic force microscopy (AFM), thioflavin T (ThT) fluorescence assay, Far-UV circular dichroism (CD) and Raman spectroscopy, and modeling the effect of succinimide-like derivative intermediates of intramolecular deamidation of the backbone during amyloid fibrillation. The AFM measurement confirmed that succinimide effectively accelerated the morphological changes of HEWL, while at the molecular level, the accelerative transformation of protein secondary structures was also clarified by ThT fluorescence assay and Far-UV CD spectroscopy. The incubation time-dependent Raman spectroscopy further revealed that the direct transformation from α-helices to organized β-sheets occurred upon skipping the intermediate random coils under the action of succinimide. This "bridge" effect of succinimide was attributed to its special influence on disulfide bonds. In the presence of succinimide in protein solutions, the native disulfide bonds of lysozyme could be broken more efficiently and quickly within hydrolysis, resulting in exposure of the buried hydrophobic residues and accelerating the formation of cross β-sheet structures. The present investigation provides very useful information for understanding the effect of intramolecular deamidation on the whole amyloid fibrillation.

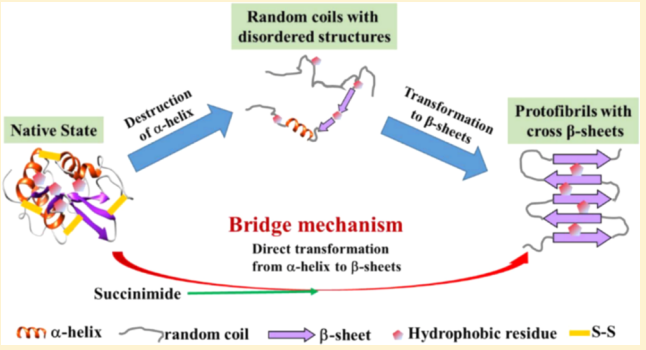

1. INTRODUCTION

The misfolded protein may cause partial loss of their functions in normal life activities.[1,2] As a typical misfolded process, amyloid fibrillation of protein can form many β-sheet-rich fibrils, leading to a series of diseases, such as Alzheimer's disease, Parkinson's disease, and Huntington's disease.[1−3] Since the amyloid fibrils are critical for human health, many efforts have been devoted to studying the amyloid fibrillation mechanism to provide useful clues.[4]

Hen egg-white lysozyme (HEWL) has 129 amino acid residues and a predominant α-helical conformation.[5] Its amyloid fibrillation is very similar to that of amyloid-β (Aβ) proteins associated with Alzheimer's disease.[6−10] Thus, HEWL has been widely used as a model protein to investigate amyloid formation mechanisms under specific experimental conditions. Recently, we have proposed a four-stage kinetic model for amyloid fibrillation of HEWL under thermal (65 °C) and acidic (pH = 2.0) conditions.[11] The partial unfolding of HEWL in the native state occurs quickly and spontaneously due to hydrolysis, followed by the conformational changes of tertiary and secondary structures. With the destruction of the predominant α-helices, many soluble oligomers with disordered structures, like annular and spherical protofibrils, are formed. Then, the soluble oligomers can finally assemble into fibrils with organized β-sheet-rich structures. In other words, the formation of organized β-sheets is a typical two-stage process from the destruction of the α-helices.[12]

It is worth noting that in the above kinetic mechanism, the soluble oligomers play a significant role of intermediates. Growing pieces of evidence showed that these small oligomers are more toxic than mature fibrils, since they can efficiently damage membrane integrity, leading to cellular stress and/or apoptosis.[13−18] Therefore, accelerating the conversion from oligomers to mature fibrils is believed to be a valuable strategy for treatment of diseases.[13−18]

According to the interactions on different kinetic stages, some small molecules are able to manipulate amyloid fibrillation of protein.[19−24] O-methylated 3HPs are able to

Received: July 22, 2019
Revised: August 27, 2019
Published: September 3, 2019

DOI: 10.1021/acs.jpcb.9b06958
J. Phys. Chem. B 2019, 123, 8057−8064

Scheme 1. Intramolecular Deamidation Mechanism of the Protein Backbone under Thermal and Acidic Conditions, Taking L-Asn for Instance

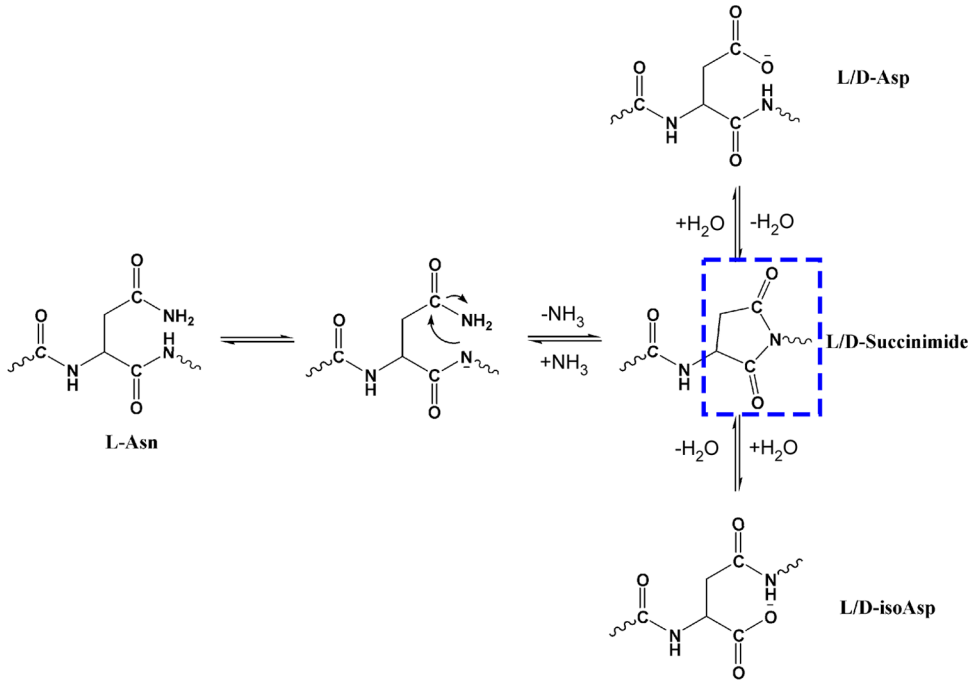

stabilize the native HEWL and hinder the fibrillogenesis owing to binding to α- and β-domains.[25] Curcumin shows an inhibition effect by inducing the decomposition of the existing protofibrils.[26] Methionine−ruthenium complexes can also inhibit hIAPP aggregation and depolymerize mature hIAPP fibrils.[27] In contrast, the influence of metal ions is more complicated.[28] On the contrary, a few small molecules can accelerate the amyloid fibrillation. Recently, fluoroquinolone drug ofloxacin has been found to be able to accelerate the formation of HEWL fibrils by inducing conformational modification of the aggregation precursor state and promoting aggregation of partially unfolded structures.[29] Orcein-related small molecule, O_4, can accelerate Aβ fibrillation by directly binding to hydrophobic amino acid residues in peptides and hence stabilizing the self-assembly of seeding components like β-sheet-rich protofibrils.[30] Polyphosphate has an ability to induce the amyloid fibrillation of β2m under acidic conditions through attractive electrostatic interactions.[31] In summary, to find more efficient accelerators is necessary for scientists to make new treatment strategies.

It is well known that the intramolecular deamidation of the protein backbone plays the special role of a trigger in amyloid fibrillation.[32−34] During deamidation as shown in Scheme 1, the peptide backbone is extended by adding one CH_2 group, accompanying the formation of a center of one negative charge.[34] Thus, the original structures of proteins are destabilized thereupon, triggering their aggregation. However, the effect of succinimide-like derivatives as intermediates of deamidation on the whole amyloid fibrillation of HEWL is unclear.

In this paper, the influence of succinimide on the formation kinetics of HEWL fibrils under thermal and acidic conditions (65 °C and pH 2.0) was carefully investigated with a combined spectroscopic approach. Upon adding succinimide into HEWL solution, the morphological changes of protein were observed from atomic force microscopy (AFM) images, whereas the thioflavin T (ThT) fluorescence assay and Far-UV circular dichroism (CD) spectroscopy clarified the influence of succinimide on the transformation of α-helices into organized β-sheets. Moreover, at the molecular level, the secondary and tertiary structural changes of aqueous lysozyme during amyloid fibrillation were measured using incubation-time-dependent Raman spectroscopy. By analyzing the kinetics of specific Raman markers, especially the stretching vibration of disulfide bonds, the action mechanism of succinimide was revealed. The present investigation clearly illuminates the unique effect of the deamidation reaction during amyloid fibrillation of HEWL.

2. EXPERIMENTAL SECTION

2.1. Protein Solutions. Hen egg-white lysozyme (activity: 22800 U/mg) was purchased from Sangon Biotech (Shanghai) Co. Ltd. Thioflavin T (ThT) and succinimide were purchased from Sinopharm Chemical Reagent Co. Ltd. They were used without further purification. An aqueous solution of HEWL (20 mg/mL) was prepared in the absence and presence of succinimide (20 mg/mL), respectively. Hydrochloric acid was used to adjust the pH value to 2.0. The prepared lysozyme solutions in sealed glass vials were incubated in a thermoshaker incubator at 65 °C without agitation. An aliquot solution of the formed fibrils was taken out of the vials at different times, and the gelatinous phase was separated by centrifugation at 12 000g for 20 min to eliminate the interference caused by protein gelation. The soluble fraction was directly used in experimental measurements of the ThT fluorescence assay, AFM, CD analysis, and Raman spectroscopy.

2.2. Atomic Force Microscopy. Protein solutions were diluted 100-fold with Milli-Q water. A 10 μL solution was dropped on freshly cleaved mica and allowed to stand for 15 min at room temperature. Then, the mica was rinsed five times with deionized water and dried with nitrogen. The AFM images of the samples on the mica were recorded under a Veeco DI-MultiMode V scanning probe microscope in the

DOI: 10.1021/acs.jpcb.9b06958
J. Phys. Chem. B 2019, 123, 8057−8064

tapping mode using a 5 μm × 5 μm scanner. All of the images were processed using the open-access software from Nanoscope Inc.

2.3. ThT Fluorescence Assay. Protein solutions were diluted 10-fold with the ThT solution (4 mg/L). Upon photoexcitation at 440 nm, the fluorescence emission within a wavelength range of 400−800 nm was dispersed and detected with a triple monochromator (TriplePro, Acton Research) equipped with a photomultiplier. The assay was performed ex situ for the mixed solution immediately. Five acquisitions were averaged to get the final intensity at various incubation times. All measurements were performed under ambient conditions.

2.4. Far-UV CD Analysis. The protein solution was diluted 100-fold. The far-UV CD spectra of the samples in 0.2 mm quartz cuvettes were measured using a J-810 Spectrophotometer (JASCO) in the wavelength range of 200−240 nm, with a bandwidth of 1 nm. The scanning speed was 100 nm/min, and the response time was 1s. All of the CD spectra were averaged at least three times.

2.5. Spontaneous Raman Spectroscopy. Spontaneous Raman spectroscopy was performed as described elsewhere.[11,35−38] Briefly, in a back-scattering geometry, a continuous-wave laser (532 nm, Verdi V5, Coherent) with 1 W power was focused on the solutions in a 10 mm × 10 mm quartz cuvette by an f = 5 cm lens, and the confocal Raman scattering was converged into a triple monochromator (TriplePro; Acton Research) through an f = 20 cm lens. The dispersed spectra were recorded using a liquid-nitrogen-cooled CCD detector (Spec-10:100B; Princeton Instruments). The Raman shifts were calibrated using the standard spectral lines of a mercury lamp. The resolution of the spectra is about 1 cm^{-1}. The acquisition time for recording spectra was approximately 1 min. At every incubation time, Raman spectra were averaged from 20 acquisitions under the same conditions and corrected by subtracting the spectra of hydrochloric acid solution measured under identical conditions.

3. RESULTS AND DISCUSSION

3.1. Morphological Changes of HEWL during Amyloid Fibrillation. Morphological changes of protein during amyloid fibrillation are visible in AFM images. Figure 1 shows the AFM images of lysozyme in the absence and presence of succinimide, at three typical incubation times. At the very early stage, no particles were observed in AFM images, since lysozyme in the native state was too small. In the absence of succinimide, spherical aggregates were gradually formed, which assembled into oligomers (Figure 1b), while the short protofibrils were formed like rods of ∼7 nm diameter as shown in Figure 1c after incubation for 96 h. In the presence of succinimide, the fibrillation process was significantly accelerated under the same conditions. The oligomers only existed for several hours, and some short protofibrils with a diameter of ∼8 nm were clearly observed in AFM images (Figure 1e) after incubation for 24 h, indicating that succinimide plays the role of an accelerator in the amyloid fibrillation of lysozyme. In addition, the morphologies of the mature fibrils in the absence and presence of succinimide were almost identical, implying that succinimide does not affect the aggregation of protofibrils, especially assembly structures.

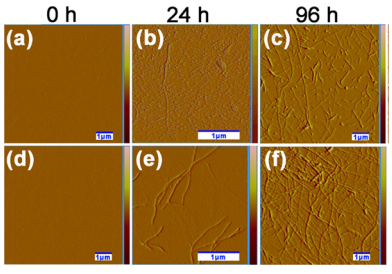

Figure 1. AFM height images of HEWL solutions incubated at 65 °C and pH 2.0 for 0 h (a), 24 h (b), and 96 h (c) in the absence of succinimide, while for 0 h (d), 24 h (e), and 96 h (f) in the presence of succinimide.

3.2. Changes of the Secondary Structure of HEWL during Amyloid Fibrillation. When ThT is added into protein solutions, its fluorescence intensity at ∼480 nm may be enhanced significantly by specially binding to β-sheet structures. Therefore, the ThT fluorescence intensity is widely used as the gold standard for quantification of the formation of organized β-sheet-rich structures during amyloid fibrillation.[39,40]

Figure 2a shows the fluorescence spectra of HEWL/ThT solutions in the absence or presence of succinimide at a few specific incubation times. For lysozyme in the native state, ThT fluorescence intensity was very weak due to the very limited population of organized β-sheets. With the increase of incubation time, the fluorescence was gradually enhanced, indicating that more and more organized β-sheet structures were formed. After incubation for 216 h, the fluorescence intensity was saturated and remained constant regardless of the existence of succinimide as shown in Figure 2a, since the mature fibrils were formed finally. However, it is worth noting that succinimide evidently accelerates the enhancement of ThT fluorescence during amyloid fibrillation, as shown in Figure 2a. After being incubated for 108 h, the fluorescence intensity was remarkably enhanced in the presence of succinimide (blue lines in Figure 2a), indicating that the organized β-sheet-rich structures were formed in advance under the action of succinimide.

To clearly show the effect of succinimide on the formation rate of organized β-sheet-rich structures, the relationship between the fluorescence intensity at 480 nm and the incubation time is plotted in Figure 2b. As suggested previously,[41−43] the curves were fitted by the sigmoid function of eq 1.

$$S = S_D + \frac{S_N - S_D}{1 + \exp[(t - t_m)/\Delta t]} \quad (1)$$

where S_N and S_D are the fluorescence intensities of the initial and final states, respectively; t is the incubation time; t_m is the transition midpoint of the sigmoid curve; and 2 × Δt represents the transition time interval. In the absence of succinimide, the midpoint was determined as 119.0 ± 6.8 h, whereas, it was accelerated to 68.2 ± 6.9 h under the action of succinimide. Moreover, the lag phase was shortened evidently too in the presence of succinimide. The results definitely confirm that succinimide effectively promotes the formation of organized β-sheet-rich structures, even from the early period. As the intermediates of intramolecular deamidation of the backbone, succinimide-like derivatives are able to disorganize the initial secondary structures of proteins.[32−34] However, the transformation from α-helices to β-sheet structures with the action of succinimide is still unclear. Far-UV CD spectroscopy

DOI: 10.1021/acs.jpcb.9b06958
J. Phys. Chem. B 2019, 123, 8057−8064

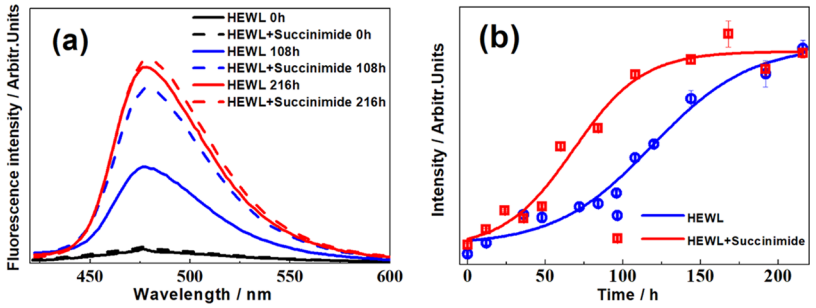

Figure 2. (a) ThT fluorescence spectra of lysozyme solution at various incubation times, in the absence (solid lines) and presence (dashed lines) of succinimide. (b) Dependence of the ThT fluorescence intensity at 480 nm on the incubation times.

is usually used to investigate the changes of secondary structures, where the intensities of the two negative peaks at 208 and 218 nm are correlated with the population ratios of α-helical and β-sheet structures, respectively.[44] Therefore, the center of the whole band consisting of the two adjacent peaks will be slightly red-shifted, accompanying the transformation from α-helices to β-sheet structures.

In the absence of succinimide, the two-dimensional CD spectrum of lysozyme under thermal and acidic conditions is shown in Figure 3a. The CD spectra exhibited a distinct dependence on incubation times. At the early stage, a distinct negative peak at 208 nm was clearly observed with a tail toward a long wavelength (Figure S1 of the Supporting Information), which was consistent with the dominant population of α-helices for lysozyme in the native state. With the incubation time, the peak at 208 nm gradually disappeared, whereas a wide peak appeared at 218 nm, indicating the transformation into β-sheet structures. It was worth noting that a ridge between the two negative peaks was formed at the incubation time of ~100 h. The phenomenon was generally consistent with the previous conclusions[45] that indirect transformation occurs from α-helices to β-sheet structures. As revealed recently from Raman spectroscopy,[11] the destruction of α-helical structures initially forms statistical coils of disordered structures, such as β-turns, loose β-strands, and polyproline structures and then thermal diffusion mediates the gradual formation of hydrogen bond networks of organized β-sheets. Based on the four-stage kinetic mechanism for amyloid fibrillation of lysozyme under thermal and acidic conditions,[11] the ridge in Figure 3a was contributed by the intermediates of assembly from protofibrils to mature fibrils.

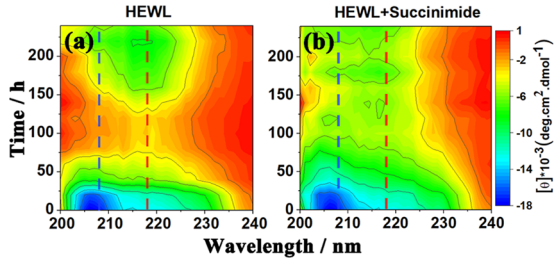

Figure 3. Two-dimensional far-UV CD spectra of lysozyme under thermal and acidic conditions in the absence (a) and presence (b) of succinimide.

However, when succinimide is added into the solutions, the ridge separating the α-helical and β-sheet structures disappeared as in Figure 3b. Although the dominant secondary structures of lysozyme in the final stage were unchanged, organized β-sheets were distinctly formed ahead, indicating that succinimide might induce the transformation from α-helices to β-sheet structures directly and shorten the period of fibrillation.

3.3. Raman Spectroscopy of HEWL during Amyloid Fibrillation. As proposed recently,[11] Raman spectroscopy is powerful to study the tertiary and secondary structural transformations under thermal and acidic conditions, since the Raman shift, scatting intensity, and/or full width at half-maximum of specific vibrational bands were very sensitive to the microenvironment of protein.[12,46−48] In the present experiments, three well-known vibrational bands were selected for quantitative analysis of denaturation of lysozyme: (1) the N−C_α−C stretching vibration at 933 cm^{-1} is closely associated with α-helical structures;[48−50] (2) the amide I band in the

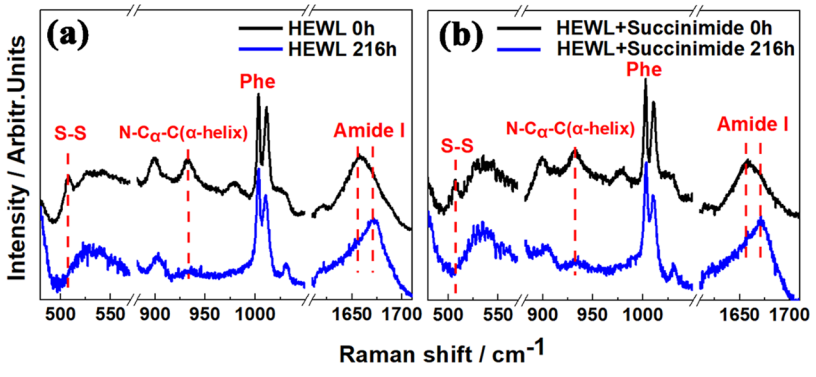

Figure 4. Raman spectra of lysozyme in the native state and the mature fibrils under thermal and acidic conditions, in the absence (a) and presence (b) of succinimide. The spectral intensities were normalized by the Phe band at 1003 cm^{-1}.

DOI: 10.1021/acs.jpcb.9b06958
J. Phys. Chem. B 2019, 123, 8057−8064

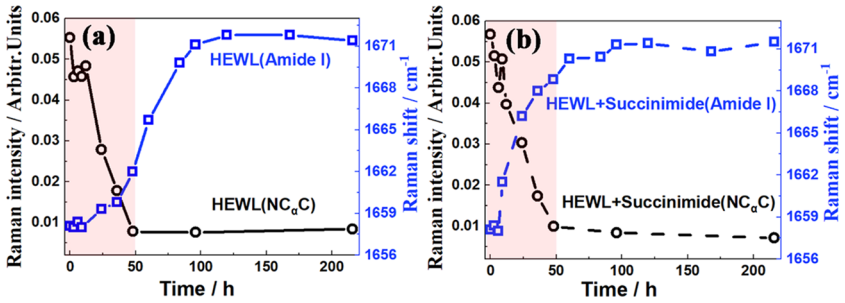

Figure 5. Time-dependent curves of the N−C$_\alpha$−C stretching band intensity at 933 cm^{-1} and the peak position of the amide I band, in the absence (a) and presence (b) of succinimide.

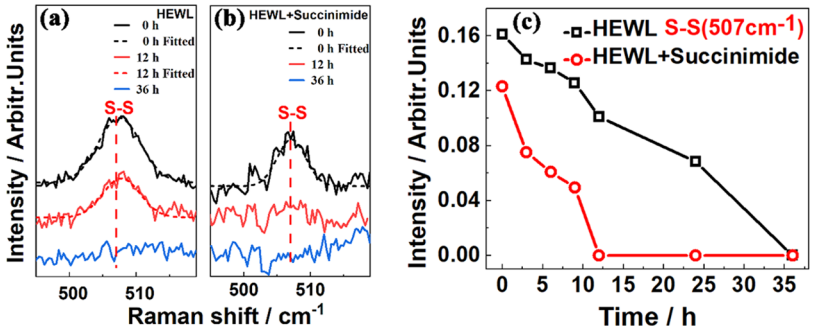

Figure 6. Magnified Raman spectra of lysozyme in the range of the S−S stretching vibration (a) in the absence of succinimide and (b) in the presence of succinimide; (c) the time-dependent curves of the band intensity at 507 cm^{-1} over the incubation time.

range of 1640−1680 cm^{-1} is contributed by various secondary structures, e.g., α-helices, disordered structures, and organized β-sheets;[51−53] (3) the stretching vibrational band of disulfide (SS) bridges is located at 507 cm^{-1}.[12,46,54]

The overall Raman spectra of lysozyme in the native state and the mature fibrils formed under thermal and acidic conditions were measured in the region from 440 to 1760 cm^{-1}. Figure 4 shows the magnified Raman spectra including the three spectral markers in the absence and presence of succinimide. Because protein concentrations in the soluble fractions were reduced due to fibril formation and gelation, intensities of all of the vibrational peaks were weaker than themselves in the native lysozyme. As suggested previously,[55−57] the spectral intensity of the Phe ring was insensitive to the microenvironment and was proportional to protein concentration. Therefore, the spectral intensities in Figure 4 were normalized by the Phe band at 1003 cm^{-1} for comparison. The spectra of the native lysozyme and the mature fibrils exhibited many evident changes, such as the wavenumber shift of the amide I band, reductions of the SS stretching, and N−C$_\alpha$−C vibrational band intensities. However, no distinct difference could be found for both the native lysozyme and the mature fibrils, regardless of in the absence or presence of succinimide, indicating that succinimide did not affect the initial and final structures of lysozyme. This was consistent with the conclusions of AFM and ThT fluorescence assay.

The detailed information of structural transformation during amyloid fibrillation can be revealed from the kinetic measurements. Figure 5 shows the dependence of the N−C$_\alpha$−C band intensity at 933 cm^{-1} on incubation time. Within the range of uncertainty, succinimide did not show an obvious improvement for destruction of α-helices, since the N−C$_\alpha$−C band intensity was almost linearly reduced to the minimum after incubation for ∼50 h.

However, a different dependence was observed for the peak position shift of the amide I band as shown in Figure 5. It is well known that the amide I band consisted of the contributions from various secondary structures of protein. Depending on the strength of the hydrogen bonding interaction (C═O···H) involving amide groups and the dipole−dipole interaction between carboxyl groups, the specific secondary structures have different frequencies: the α-helical structure usually contributes the spectral intensity in the 1640−1660 cm^{-1} range;[58,59] the organized β-sheets are located in the range of 1660−1680 cm^{-1};[52,60,61] and the disordered structures, such as β-turns, loose β-strands, and polyproline structures, have resonance frequencies of lower than 1640 cm^{-1} or higher than 1680 cm^{-1}.[48,58] Therefore, when the organized β-sheets are dominantly formed, the amide I position is expected to be blue-shifted. Indeed, a blue shift of 12 cm^{-1} was observed in Figure 4, which was consistent with that the dominant secondary structures of mature fibrils were organized β-sheets.

It is worth noting that the formation rate of organized β-sheet structures was visibly accelerated in the presence of succinimide. In the solution without adding succinimide, the peak position started to blue-shift after incubation for ∼20 h, and only a 4 cm^{-1} shift was observed for the amide I peak 50 h later. The whole blue shift of 12 cm^{-1} was achieved at ∼90 h. The relative delay from the destruction of α-helices to the formation of cross β-sheets agreed very well with the step-by-step transformation mechanism of secondary structural changes.[11] In contrast, under the action of succinimide, a visible shift of the amide I peak was observed when being incubated for only ∼10 h and it reached its maximum after 60 h. The spectral evidence definitely confirmed that succinimide

DOI: 10.1021/acs.jpcb.9b06958
J. Phys. Chem. B 2019, 123, 8057−8064

plays the role of an efficient accelerator to form organized β-sheet structures, which is also consistent with the conclusions of our CD spectra and ThT fluorescence assay.

3.4. Action Mechanism of Succinimide. As deamidation intermediates, succinimide-like derivatives can naturally affect the destruction and transformation of secondary structures of protein. To further reveal the action mechanism of succinimide, the secondary bonds for stabilizing protein structures, such as the disulfide bonds formed between the thiol groups of cysteine residues, are checked carefully. Therefore, the Raman band at 507 cm^{-1} was quantitatively analyzed during amyloid fibrillation of HEWL, which is associated with the stretching vibration of disulfide (S−S) bridges.[12] It is well known that the disulfide bonds play vital roles in protein stability and their disruptions usually destabilize the original structures in the native state.[62] Additionally, local hydrophobic residues condense around the disulfide bonds through hydrophobic interactions to form the nucleus of a hydrophobic core of the folded protein,[63−66] which may prevent the influences of water and other interactive groups. Thus, when the disulfide bonds are broken, the hydrophobic residues are exposed to an aqueous environment, preferring the formation of cross β-sheets or β-turns.[44,67]

Figure 6a,b show the partially magnified Raman spectra of lysozyme in the range of the S−S stretching vibration, in the absence and presence of succinimide, respectively, under thermal and acidic conditions. Obviously, the band intensity was gradually reduced regardless of the existence of succinimide, reflecting reduction of the number of disulfide bonds. Figure 6c plots the dependent curves of the bond intensity at 507 cm^{-1} over incubation times. At the beginning, the number of disulfide bonds was reduced to a certain extent due to the action of succinimide. It is understandable because the addition of succinimide into solutions implies the partial occurrence of deamidation. With the increase of incubation time, the number of disulfide bonds in the solutions was decreased in the presence of succinimide much quickly than the case without adding succinimide. To our surprise, the periods of the disulfide bond reduction were exactly in agreement with the starting points of formation of the organized β-sheets (Figure 5), e.g., ∼10 h in the presence of succinimide and ∼35 h in its absence. Therefore, the action mechanism of succinimide can be illuminated: with the addition of succinimide into protein solutions, a negatively charged center produced by the hydration of succinimide can induce the looseness of protein structures by the attractive electrostatic interaction with the positively charged amino acids. Thus, the disulfide bonds are broken and the hydrolysis of the backbone is significantly promoted. As a result, the hydrophobic residues that condensed around the disulfide bonds are exposed to an aqueous environment, leading to the direct formation of cross β-sheets or β-turns. In other words, organized β-sheets can be formed upon skipping the formation of intermediate random coils.

Since the amyloid fibrillation of lysozyme under thermal and acidic conditions is a highly complex process, involving hydrolysis, deamidation, transformation of secondary structures, and so on, the influence of succinimide might exist in all of the stages. However, based on the present experiments, succinimide seems to dominantly accelerate the formation of the organized β-sheets during amyloid fibrillation of lysozyme. The diagram in Scheme 2 briefly describes the role of succinimide. In the absence of succinimide, the intermediate random coils with disordered structures are first formed by the destruction of α-helices, which then gradually transform into organized β-sheet structures. In contrast, a bridge is built by succinimide between the α-helices and the organized β-sheet structures, which makes the direct transformation into organized β-sheets feasible upon skipping the intermediate random coils.

Scheme 2. Schematic Diagram of the "Bridge" Role of Succinimide during Amyloid Fibrillation

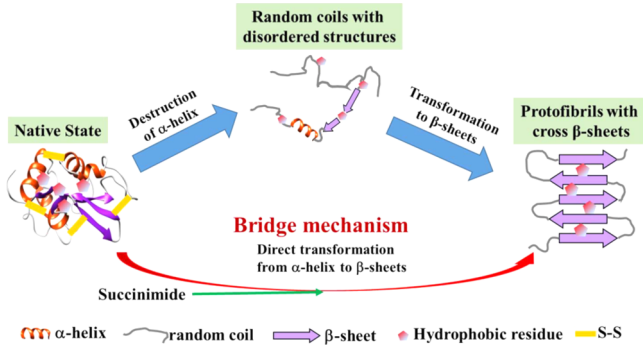

4. CONCLUSIONS

In this study, we investigated the influence of succinimide on amyloid fibrillation of HEWL under thermal and acidic conditions with a combination of several experimental techniques. The morphological changes of HEWL toward fibrils were effectively accelerated by succinimide as observed in AFM images. The ThT fluorescence assay and Far-UV CD spectroscopy confirmed that this acceleration at the molecular level was associated with the promotion on the formation rate of organized β-sheets. Of note, the lifetime of the soluble oligomers with disordered structures was dramatically reduced in the presence of succinimide, as the ridge between α-helical and β-sheet secondary structures disappears in two-dimensional CD spectra, implying the direct formation of organized β-sheets upon hydrolysis.

For understanding the action mechanism of succinimide, incubation-time-dependent Raman spectra were recorded in the range of 440−1760 cm^{-1}, especially for three well-known Raman markers, e.g., the N−C_α−C stretching vibration at 933 cm^{-1}, the amide I band, and the S−S stretching band at 507 cm^{-1}. Both the spectral markers (the N−C_α−C and amide I peaks) of the protein backbone showed the influence of succinimide on the transformation of secondary structures during fibrillation. In the absence of succinimide, the α-helical structures preferentially transformed into random coils with disordered structures and then gradually converted to organized β-sheets. Within the process, these random coils could aggregate into soluble oligomers, leading to cellular toxicity.

Additionally, the spectral analysis of the S−S stretching peak intensity at 507 cm^{-1} suggested that succinimide had a strong influence on the destruction of disulfide bands. In the presence of succinimide, the native disulfide bonds of lysozyme can be broken more efficiently by hydrolysis, consequently resulting in exposure of the buried hydrophobic residues and accelerating the direct formation of organized β-sheet structures. In other words, succinimide plays a bridge role to promote the direct transformation into organized β-sheets upon skipping the

DOI: 10.1021/acs.jpcb.9b06958
J. Phys. Chem. B 2019, 123, 8057−8064

intermediate random coils. As a result, the number of soluble oligomers and protofibrils with relatively high toxic levels can be significantly reduced. Therefore, the present investigation provides very useful information for developing new medicines for neurodegenerative diseases by accelerating fibrillation.

■ ASSOCIATED CONTENT

Supporting Information

The Supporting Information is available free of charge on the ACS Publications website at DOI: 10.1021/acs.jpcb.9b06958.

Far-UV CD spectra of lysozyme at various incubation times in the absence and presence of succinimide (PDF)

■ AUTHOR INFORMATION

Corresponding Authors

*E-mail: xzhou@ustc.edu.cn (X.Z.).
*E-mail: yyq@ahu.edu.cn (Y.Y.).
*E-mail: slliu@ustc.edu.cn (S.L.).

ORCID

Xiaoguo Zhou: 0000-0002-0264-0146
Yuanqin Yu: 0000-0001-7647-8404

Notes

The authors declare no competing financial interest.

■ ACKNOWLEDGMENTS

This work was supported by the National Natural Science Foundation of China (Grant Nos 21573208, 21573210, 21873089, and 21873002) and the National Key Basic Research Foundation of China (Grant No. 2013CB834602).

■ REFERENCES

(1) Uversky, V. N.; Fink, A. L. Conformational constraints for amyloid fibrillation: the importance of being unfolded. *Biochim. Biophys. Acta, Proteins Proteomics* **2004**, *1698*, 131−153.
(2) Chiti, F.; Dobson, C. M. Protein misfolding, functional amyloid, and human disease. *Annu. Rev. Biochem.* **2006**, *75*, 333−366.
(3) Dobson, C. M. Principles of protein folding, misfolding and aggregation. *Semin. Cell Dev. Biol.* **2004**, *15*, 3−16.
(4) Roberts, C. J. Protein aggregation and its impact on product quality. *Curr. Opin. Biotechnol.* **2014**, *30*, 211−217.
(5) Vaney, M.; Maignan, S.; Ries-Kautt, M.; Ducruix, A. High-resolution structure (1.33 Å) of a HEW lysozyme tetragonal crystal grown in the APCF apparatus. Data and structural comparison with a crystal grown under microgravity from SpaceHab-01 mission. *Acta Crystallogr., Sect. D: Biol. Crystallogr.* **1996**, *52*, 505−517.
(6) Booth, D. R.; Sunde, M.; Bellotti, V.; Robinson, C. V.; Hutchinson, W. L.; Fraser, P. E.; Hawkins, P. N.; Dobson, C. M.; Radford, S. E.; Blake, C. C. Instability, unfolding and aggregation of human lysozyme variants underlying amyloid fibrillogenesis. *Nature* **1997**, *385*, 787−793.
(7) Frare, E.; Polverino De Laureto, P.; Zurdo, J.; Dobson, C. M.; Fontana, A. A highly amyloidogenic region of hen lysozyme. *J. Mol. Biol.* **2004**, *340*, 1153−1165.
(8) Swaminathan, R.; Ravi, V. K.; Kumar, S.; Kumar, M. V. S.; Chandra, N. Lysozyme: a model protein for amyloid research. *Adv. Protein Chem. Struct. Biol.* **2011**, *84*, 63−111.
(9) Zou, Y.; Hao, W.; Li, H.; Gao, Y.; Sun, Y.; Ma, G. New insight into amyloid fibril formation of hen egg white lysozyme using a two-step temperature-dependent FTIR approach. *J. Phys. Chem. B* **2014**, *118*, 9834−9843.
(10) Ma, B.; Zhang, F.; Wang, X.; Zhu, X. Investigating the inhibitory effects of zinc ions on amyloid fibril formation of hen egg-white lysozyme. *Int. J. Biol. Macromol.* **2017**, *98*, 717−722.
(11) Xing, L.; Fan, W.; Chen, N.; Li, M.; Zhou, X.; Liu, S. Amyloid formation kinetics of hen egg white lysozyme under heat and acidic conditions revealed by Raman spectroscopy. *J Raman Spectrosc.* **2019**, *50*, 629−640.
(12) Xing, L.; Lin, K.; Zhou, X.; Liu, S.; Luo, Y. Multistate mechanism of lysozyme denaturation through synchronous analysis of Raman spectra. *J. Phys. Chem. B* **2016**, *120*, 10660−10667.
(13) Caughey, B.; Lansbury, P. T. Protofibrils, pores, fibrils, and neurodegeneration: separating the responsible protein aggregates from the innocent bystanders. *Annu. Rev. Neurosci.* **2003**, *26*, 267−298.
(14) Chong, Y. H.; Shin, Y. J.; Lee, E. O.; Kayed, R.; Glabe, C. G.; Tenner, A. J. ERK1/2 activation mediates Abeta oligomer-induced neurotoxicity via caspase-3 activation and tau cleavage in rat organotypic hippocampal slice cultures. *J. Biol. Chem.* **2006**, *281*, 20315−20325.
(15) Lansbury, P. T.; Lashuel, H. A. A century-old debate on protein aggregation and neurodegeneration enters the clinic. *Nature* **2006**, *443*, 774−779.
(16) Walsh, D. M.; Selkoe, D. J. Aβ oligomers−a decade of discovery. *J. Neurochem.* **2007**, *101*, 1172−1184.
(17) Cizas, P.; Budvytyte, R.; Morkuniene, R.; Moldovan, R.; Broccio, M.; Losche, M.; Niaura, G.; Valincius, G.; Borutaite, V. Size-dependent neurotoxicity of beta-amyloid oligomers. *Arch. Biochem. Biophys.* **2010**, *496*, 84−92.
(18) Kayed, R.; Lasagna-Reeves, C. A. Molecular mechanisms of amyloid oligomers toxicity. *J. Alzheimer's Dis.* **2013**, *33*, S67−S78.
(19) Cohen, F. E.; Kelly, J. W. Therapeutic approaches to protein-misfolding diseases. *Nature* **2003**, *426*, 905−909.
(20) Herbst, M.; Wanker, E. E. Therapeutic approaches to polyglutamine diseases: combating protein misfolding and aggregation. *Curr. Pharm. Des.* **2006**, *12*, 2543−2555.
(21) Bai, C.; Lin, D.; Mo, Y.; Lei, J.; Sun, Y.; Xie, L.; Yang, X.; Wei, G. Influence of fullerenol on hIAPP aggregation: amyloid inhibition and mechanistic aspects. *Phys. Chem. Chem. Phys.* **2019**, *21*, 4022−4031.
(22) Mohammad-Beigi, H.; Aliakbari, F.; Sahin, C.; Lomax, C.; Tawfike, A.; Schafer, N. P.; Amiri-Nowdijeh, A.; Eskandari, H.; Moller, I. M.; Hosseini-Mazinani, M.; et al. Oleuropein derivatives from olive fruit extracts reduce alpha-synuclein fibrillation and oligomer toxicity. *J. Biol. Chem.* **2019**, *294*, 4215−4232.
(23) Mudedla, S. K.; Murugan, N. A.; Subramanian, V.; Agren, H. Destabilization of amyloid fibrils on interaction with MoS2-based nanomaterials. *RSC Adv.* **2019**, *9*, 1613−1624.
(24) Saelices, L.; Nguyen, B. A.; Chung, K.; Wang, Y.; Ortega, A.; Lee, J. H.; Coelho, T.; Bijzet, J.; Benson, M. D.; Eisenberg, D. S. A pair of peptides inhibits seeding of the hormone transporter transthyretin into amyloid fibrils. *J. Biol. Chem.* **2019**, *294*, 6130−6141.
(25) Mariño, L.; Pauwels, K.; Casasnovas, R.; Sanchis, P.; Vilanova, B.; Munoz, F.; Donoso, J.; Adrover, M. Ortho-methylated 3-hydroxypyridines hinder hen egg-white lysozyme fibrillogenesis. *Sci. Rep.* **2015**, *5*, No. 12052.
(26) Wang, S. S.; Liu, K. N.; Lee, W. H. Effect of curcumin on the amyloid fibrillogenesis of hen egg-white lysozyme. *Biophys. Chem.* **2009**, *144*, 78−87.
(27) Gong, G.; Xu, J.; Huang, X.; Du, W. Influence of methionine-ruthenium complex on the fibril formation of human islet amyloid polypeptide. *J. Biol. Inorg. Chem.* **2019**, *24*, 179−189.
(28) Xing, L.; Chen, N.; Fan, W.; Li, M. N.; Zhou, X. G.; Liu, S. L. Double-edged effects of aluminium ions on amyloid fibrillation of hen egg-white lysozyme. *Int. J. Biol. Macromol.* **2019**, *132*, 929−938.
(29) Muthu, S. A.; Mothi, N.; Shiriskar, S. M.; Pissurlenkar, R. R.; Kumar, A.; Ahmad, B. Physical basis for the ofloxacin-induced acceleration of lysozyme aggregation and polymorphism in amyloid fibrils. *Arch. Biochem. Biophys.* **2016**, *592*, 10−19.
(30) Bieschke, J.; Herbst, M.; Wiglenda, T.; Friedrich, R. P.; Boeddrich, A.; Schiele, F.; Kleckers, D.; Lopez del Amo, J. M.; Gruning, B. A.; Wang, Q.; et al. Small-molecule conversion of toxic

DOI: 10.1021/acs.jpcb.9b06958
J. Phys. Chem. B 2019, 123, 8057−8064

oligomers to nontoxic beta-sheet-rich amyloid fibrils. *Nat. Chem. Biol.* **2011**, *8*, 93−101.
(31) Zhang, C. M.; Yamaguchi, K.; So, M.; Sasahara, K.; Ito, T.; Yamamoto, S.; Narita, I.; Kardos, J.; Naiki, H.; Goto, Y. Possible mechanisms of polyphosphate-induced amyloid fibril formation of beta2-microglobulin. *Proc. Natl. Acad. Sci. U.S.A.* **2019**, *116*, 12833−12838.
(32) Takata, T.; Oxford, J. T.; Demeler, B.; Lampi, K. J. Deamidation destabilizes and triggers aggregation of a lens protein, betaA3-crystallin. *Protein. Sci.* **2008**, *17*, 1565−1575.
(33) Shimizu, T.; Watanabe, A.; Ogawara, M.; Mori, H.; Shirasawa, T. Isoaspartate formation and neurodegeneration in Alzheimer's disease. *Arch. Biochem. Biophys.* **2000**, *381*, 225−234.
(34) Dunkelberger, E. B.; Buchanan, L. E.; Marek, P.; Cao, P.; Raleigh, D. P.; Zanni, M. T. Deamidation accelerates amyloid formation and alters amylin fiber structure. *J. Am. Chem. Soc.* **2012**, *134*, 12658−12667.
(35) Lin, K.; Zhou, X. G.; Liu, S. L.; Luo, Y. Identification of free OH and its implication on structural changes of liquid water. *Chin.. J. Chem. Phys.* **2013**, *26*, 121−126.
(36) Chen, L.; Zhu, W. D.; Lin, K.; Hu, N. Y.; Yu, Y. Q.; Zhou, X. G.; Yuan, L. F.; Hu, S. M.; Luo, Y. Identification of alcohol conformers by Raman spectra in the C-H stretching region. *J. Phys. Chem. A* **2015**, *119*, 3209−3217.
(37) Yu, Y. Q.; Fan, W.; Wang, Y. X.; Zhou, X. G.; Sun, J.; Liu, S. L. Probe of alcohol structures in the gas and liquid states using C−H Stretching Raman spectroscopy. *Sensors* **2018**, *18*, 2061−2076.
(38) Yu, Y. Q.; Fan, W.; Wang, Y. X.; Zhou, X. G.; Sun, J.; Liu, S. L. C−H··· O interaction in methanol−water solution revealed from Raman spectroscopy and theoretical calculations. *J. Phys. Chem. B* **2017**, *121*, 8179−8187.
(39) Levine, H. Thioflavine T interaction with synthetic Alzheimer's disease β-amyloid peptides: detection of amyloid aggregation in solution. *Protein Sci.* **1993**, *2*, 404−410.
(40) Levine, H. Quantification of β-sheet amyloid fibril structures with thioflavin T. *Methods Enzymol.* **1999**, *309*, 274−284.
(41) Nielsen, L.; Khurana, R.; Coats, A.; Frokjaer, S.; Brange, J.; Vyas, S.; Uversky, V. N.; Fink, A. L. Effect of environmental factors on the kinetics of insulin fibril formation: elucidation of the molecular mechanism. *Biochemistry* **2001**, *40*, 6036−6046.
(42) Hédoux, A.; Willart, J. F.; Ionov, R.; Affouard, F.; Guinet, Y.; Paccou, L.; Lerbret, A.; Descamps, M. Analysis of sugar bioprotective mechanisms on the thermal denaturation of lysozyme from Raman scattering and differential scanning calorimetry investigations. *J. Phys. Chem. B* **2006**, *110*, 22886−22893.
(43) Van Stokkum, I. H. M.; Linsdell, H.; Hadden, J. M.; Haris, P. I.; Chapman, D.; Bloemendal, M. Temperature-induced changes in protein structures studied by Fourier transform infrared spectroscopy and global analysis. *Biochemistry* **1995**, *34*, 10508−10518.
(44) Ahmad, B.; Winkelmann, J.; Tiribilli, B.; Chiti, F. Searching for conditions to form stable protein oligomers with amyloid-like characteristics: The unexplored basic pH. *Biochim. Biophys. Acta, Proteins Proteomics* **2010**, *1804*, 223−234.
(45) Shashilov, V.; Xu, M.; Ermolenkov, V. V.; Fredriksen, L.; Lednev, I. K. Probing a fibrillation nucleus directly by deep ultraviolet Raman spectroscopy. *J. Am. Chem. Soc.* **2007**, *129*, 6972−6973.
(46) Wen, Z. Q. Raman spectroscopy of protein pharmaceuticals. *J. Pharm. Sci.* **2007**, *96*, 2861−2878.
(47) Tinti, A.; Di Foggia, M.; Taddei, P.; Torreggiani, A.; Dettin, M.; Fagnano, C. Vibrational study of auto-assembling oligopeptides for biomedical applications. *J. Raman Spectrosc.* **2008**, *39*, 250−259.
(48) Kocherbitov, V.; Latynis, J.; Misiunas, A.; Barauskas, J.; Niaura, G. Hydration of lysozyme studied by Raman spectroscopy. *J. Phys. Chem. B* **2013**, *117*, 4981−4992.
(49) Frushour, B.; Koenig, J. Raman spectroscopic study of tropomyosin denaturation. *Biopolymers* **1974**, *13*, 1809−1819.
(50) Frushour, B.; Koenig, J. Raman studies of the crystalline, solution, and alkaline-denatured states of β-lactoglobulin. *Biopolymers* **1975**, *14*, 649−662.
(51) Hamley, I. W. Peptide fibrillization. *Angew. Chem., Int. Ed.* **2007**, *46*, 8128−8147.
(52) Xu, M.; Shashilov, V.; Lednev, I. K. Probing the cross-beta core structure of amyloid fibrils by hydrogen-deuterium exchange deep ultraviolet resonance Raman spectroscopy. *J. Am. Chem. Soc.* **2007**, *129*, 11002−11003.
(53) Popova, L. A.; Kodali, R.; Wetzel, R.; Lednev, I. K. Structural variations in the cross-beta core of amyloid beta fibrils revealed by deep UV resonance Raman spectroscopy. *J. Am. Chem. Soc.* **2010**, *132*, 6324−6328.
(54) Sugeta, H.; Go, A.; Miyazawa, T. Vibrational spectra and molecular conformations of dialkyl disulfides. *Bull. Chem. Soc. Jpn.* **1973**, *46*, 3407−3411.
(55) Howell, N.; Li-Chan, E. Elucidation of interactions of lysozyme with whey proteins by Raman spectroscopy. *Int. J. Food. Sci. Technol.* **1996**, *31*, 439−451.
(56) Herrero, A. M.; Cambero, M. I.; Ordonez, J. A.; de la Hoz, L.; Carmona, P. Raman spectroscopy study of the structural effect of microbial transglutaminase on meat systems and its relationship with textural characteristics. *Food. Chem.* **2008**, *109*, 25−32.
(57) Herrero, A. M.; Carmona, P.; Cofrades, S.; Jiménez-Colmenero, F. Raman spectroscopic determination of structural changes in meat batters upon soy protein addition and heat treatment. *Food. Res. Int.* **2008**, *41*, 765−772.
(58) Spiro, T. G.; Gaber, B. P. Laser Raman scattering as a probe of protein structure. *Annu. Rev. Biochem.* **1977**, *46*, 553−570.
(59) Rygula, A.; Majzner, K.; Marzec, K. M.; Kaczor, A.; Pilarczyk, M.; Baranska, M. Raman spectroscopy of proteins: a review. *J. Raman Spectrosc.* **2013**, *44*, 1061−1076.
(60) Shashilov, V. A.; Xu, M.; Ermolenkov, V. V.; Lednev, I. K. Latent variable analysis of Raman spectra for structural characterization of proteins. *J. Quant. Spectrosc. Radiat. Transfer* **2006**, *102*, 46−61.
(61) Shashilov, V. A.; Lednev, I. K. 2D correlation deep UV resonance Raman spectroscopy of early events of lysozyme fibrillation: Kinetic mechanism and potential interpretation pitfalls. *J. Am. Chem. Soc.* **2008**, *130*, 309−317.
(62) Trivedi, M. V.; Laurence, J. S.; Siahaan, T. J. The role of thiols and disulfides on protein stability. *Curr. Protein Pept. Sci.* **2009**, *10*, 614−625.
(63) Li, Y.; Yan, J.; Zhang, X.; Huang, K. Disulfide bonds in amyloidogenesis diseases related proteins. *Proteins* **2013**, *81*, 1862−1873.
(64) Wineman-Fisher, V.; Tudorachi, L.; Nissim, E.; Miller, Y. The removal of disulfide bonds in amylin oligomers leads to the conformational change of the 'native' amylin oligomers. *Phys. Chem. Chem. Phys* **2016**, *18*, 12438−12442.
(65) Harpaz, Y.; Gerstein, M.; Chothia, C. Volume changes on protein folding. *Structure* **1994**, *2*, 641−649.
(66) Wedemeyer, W. J.; Welker, E.; Narayan, M.; Scheraga, H. A. Disulfide bonds and protein folding. *Biochemistry* **2000**, *39*, 4207−4216.
(67) Rochet, J.-C. Novel therapeutic strategies for the treatment of protein-misfolding diseases. *Expert Rev. Mol. Med.* **2007**, *9*, 1−34.

DOI: 10.1021/acs.jpcb.9b06958
J. Phys. Chem. B 2019, 123, 8057−8064